

A three dimensional implicit immersed boundary method with application

Jian Hao^{1,2} and Luoding Zhu^{1, a)}

¹⁾Department of Mathematical Sciences and Center for Mathematical Biosciences Indiana University - Purdue University, Indianapolis, IN 46202, USA

²⁾Department of Mathematics and Center for Research in Scientific Computation, North Carolina State University, Raleigh, NC 27695, USA

(Received 20 August 2011; accepted 26 September 2011; published online 10 November 2011)

Abstract Most algorithms of the immersed boundary method originated by Peskin are explicit when it comes to the computation of the elastic forces exerted by the immersed boundary to the fluid. A drawback of such an explicit approach is a severe restriction on the time step size for maintaining numerical stability. An implicit immersed boundary method in two dimensions using the lattice Boltzmann approach has been proposed. This paper reports an extension of the method to three dimensions and its application to simulation of a massive flexible sheet interacting with an incompressible viscous flow. © 2011 The Chinese Society of Theoretical and Applied Mechanics. [doi:10.1063/2.1106202]

Keywords immersed boundary method, lattice-Boltzmann method, implicit schemes, fluid-structure-interaction, bi-stability, flag-in-wind

The immersed boundary (IB) method pioneered by Peskin¹ is both a novel mathematical formulation and an efficient numerical method for compliant-structure-viscous-fluid interaction problems. The IB method has been successfully applied to many such problems: platelet aggregation, sperm motility, insect flight, ciliary beating, nutrient transport, valveless pumping, lamprey swimming, motions of foam and vesicles, blood flows in the human artery and heart, etc.

Most IB methods adopt an explicit approach to calculate the elastic forces on the known configuration of the structure at each time step. Since the fluid-structure-interaction is in nature a stiff problem, an explicit IB method suffers a severe restriction on time step size.^{1,2} The time step must be sufficiently small to maintain numerical stability.³⁻⁵ To overcome the inherent stiffness in the fluid-structure-interaction problems, implicit numerical methods are usually desired. Much effort has been made along this line in recent years to develop implicit or semi-implicit IB methods.⁶⁻¹⁴ However, most of these implicit methods are not practical for real application problems.^{9,11} Very recently the authors have developed a lattice-Boltzmann based two dimensional (2D) implicit immersed boundary method.¹⁵ It has been shown numerically that the proposed 2D implicit method is much more stable with larger time steps and significantly outperforms the explicit version of the IB method in terms of computational cost.

In this letter we report an extension of the previous 2D implicit IB method via the lattice-Boltzmann approach to three dimensions with application to simulation of a compliant sheet interacting with a flowing viscous fluid. Our three dimensional (3D) implicit IB method can handle massive immersed boundaries via

the d'Alembert force which only works through an implicit implementation.¹⁶

The lattice Boltzmann method¹⁷ is an alternative approach for solving the Navier-Stokes equations. It is second order accurate in both time and space, and is computationally efficient, especially for 3D problems. There exist many works coupling the lattice-Boltzmann method to the IB method, such as Refs. 18-21. However, all of the existing hybrid methods are explicit; but ours is implicit. As expected the IB approach substantially reduces the computational cost in solving the incompressible Navier-Stokes equations which renders our 3D implicit IB method appropriate for practical applications.

In our implicit IB method, the elastic force calculation is based on the unknown configuration of the structure at the next time step. Consequently a highly nonlinear algebraic system needs to be solved at each time step. In our work the nonlinear system is solved by a Jacobian-free inexact Newton-Krylov method.²² The new implicit method is applied to simulate the interaction of a flexible sheet with a viscous incompressible flow. Our preliminary results show that the fluid-sheet system exhibits two stable states — static and flapping, and the sheet mass is critical for the self-sustained flapping. All of these results are consistent with existing literatures.²³⁻²⁶

Suppose we have a compliant boundary immersed in a viscous incompressible flow. Choosing appropriate reference quantities for length, velocity and mass density, we formulate our lattice-Boltzmann IB formulation in three dimensions in dimensionless form as follows

$$\frac{\partial g(\mathbf{x}, \boldsymbol{\xi}, t)}{\partial t} + \boldsymbol{\xi} \cdot \frac{\partial g(\mathbf{x}, \boldsymbol{\xi}, t)}{\partial \mathbf{x}} + \mathbf{f}(\mathbf{x}, t) \cdot \frac{\partial g(\mathbf{x}, \boldsymbol{\xi}, t)}{\partial \boldsymbol{\xi}} = -\frac{1}{\tau}(g(\mathbf{x}, \boldsymbol{\xi}, t) - g^{(0)}(\mathbf{x}, \boldsymbol{\xi}, t)), \quad (1)$$

^{a)}Corresponding author. Email: lzhu@math.iupui.edu.

The function $g(\mathbf{x}, \boldsymbol{\xi}, t)$ is the single particle velocity distribution function, where \mathbf{x} is the spatial coordinate, $\boldsymbol{\xi}$ is the particle velocity, and t is the time. The term $-(g - g^{(0)})/\tau$ is the Bhatnagar-Gross-Krook (BGK) approximation to the complex collision operator in the Boltzmann equation, where τ is the relaxation time. The $g^{(0)}$ is the Maxwellian distribution. The external force term $\mathbf{f}(\mathbf{x}, t) = \mathbf{f}_{\text{ib}}(\mathbf{x}, t) + \mathbf{f}_{\text{d}}(\mathbf{x}, t) + \mathbf{f}_{\text{ext}}(\mathbf{x}, t)$. The $\mathbf{f}_{\text{ib}}(\mathbf{x}, t)$ is the force imparted by the immersed boundary to the fluid. The $\mathbf{f}_{\text{ext}}(\mathbf{x}, t)$ is other external forces acting on the fluid, e.g. the gravity. The $\mathbf{f}_{\text{d}}(\mathbf{x}, t)$ is the d'Alembert force due to the sheet mass. The fluid mass density (ρ) and momentum ($\rho\mathbf{u}$) may be computed from the g function by the standard approach. The Eulerian elastic force density $\mathbf{f}_{\text{ib}}(\mathbf{x}, t)$ defined on the fixed Eulerian lattice is calculated from the Lagrangian force density $\mathbf{F}(\boldsymbol{\alpha}, t)$ defined on the Lagrangian grid as follows

$$\mathbf{f}_{\text{ib}}(\mathbf{x}, t) = \int \mathbf{F}_{\text{ib}}(\boldsymbol{\alpha}, t) \delta(\mathbf{x} - \mathbf{X}(\boldsymbol{\alpha}, t)) d\boldsymbol{\alpha}, \quad (2)$$

where the function $\delta(\mathbf{x})$ is the Dirac δ -function. The Lagrangian elastic force density \mathbf{F}_{ib} is computed from the elastic potential energy density of the immersed boundary as in the standard IB method.¹⁶ The Eulerian density of the d'Alembert force $\mathbf{f}_{\text{d}}(\mathbf{x}, t)$ is computed from the corresponding Lagrangian density $\mathbf{F}_{\text{d}}(\boldsymbol{\alpha}, t)$ by the same way as computing elastic force \mathbf{f}_{ib} ,

$$\mathbf{f}_{\text{d}}(\mathbf{x}, t) = \int \mathbf{F}_{\text{d}}(\boldsymbol{\alpha}, t) \delta(\mathbf{x} - \mathbf{X}(\boldsymbol{\alpha}, t)) d\boldsymbol{\alpha}, \quad (3)$$

where the d'Alembert force $\mathbf{F}_{\text{d}}(\boldsymbol{\alpha}, t)$ is computed by definition as follows

$$\mathbf{F}_{\text{d}}(\boldsymbol{\alpha}, t) = -M(\boldsymbol{\alpha}, t) \frac{\partial^2 \mathbf{X}(\boldsymbol{\alpha}, t)}{\partial t^2}. \quad (4)$$

The motion of the immersed structure is described by a system of 1st-order ordinary differential equations

$$\frac{\partial \mathbf{X}}{\partial t}(\boldsymbol{\alpha}, t) = \mathbf{U}(\boldsymbol{\alpha}, t). \quad (5)$$

The $\mathbf{X}(\boldsymbol{\alpha}, t)$ is the Eulerian coordinate of the immersed structure at time t whose Lagrangian coordinate is $\boldsymbol{\alpha}$. The immersed boundary velocity $\mathbf{U}(\boldsymbol{\alpha}, t)$ is interpolated from the fluid velocity $\mathbf{u}(\mathbf{x}, t)$ by the same δ -function as used to convert the force from the boundary to the fluid,

$$\mathbf{U}(\boldsymbol{\alpha}, t) = \int \mathbf{u}(\mathbf{x}, t) \delta(\mathbf{x} - \mathbf{X}(\boldsymbol{\alpha}, t)) d\mathbf{x}. \quad (6)$$

The above non-linear system of integro-differential equations (Eqs. (1)–(6)) is discretized on a uniform fixed Eulerian square lattice for the fluid with the uniform mesh width h (the number of grid nodes is N_x , N_y and N_z in x , y and z direction, respectively), plus a collection of moving Lagrangian discrete points for the immersed boundary with mesh width $\Delta\alpha_1 = \Delta\alpha_2 \simeq h/2$. The D3Q19 model is used to discretize the BGK equation (1). The external forcing term in the equation is treated by the methods proposed in Refs. 4, 7.

The main idea of our 3D implicit algorithm is as follows. Let \mathcal{F} denote the operator acting on the configuration $\mathbf{X}(\boldsymbol{\alpha}, t + 1)$ to produce the Lagrangian elastic force density, \mathcal{S} denote the spreading operator of Lagrangian force density to fluid lattice, \mathcal{L} denote the operator to advance the velocity distribution function from n to $n + 1$, \mathcal{U} denote the operator to recover fluid velocity from distribution function, \mathcal{I} denote the operator to interpolate the immersed boundary velocity from the fluid, then the non-linear algebraic equation system (after g^{n+1} is eliminated) for advancing the solutions from n to $n + 1$ is given by

$$\mathcal{U}\mathcal{L}\mathcal{S}\mathcal{F}\mathbf{X}^{n+1} = \mathbf{X}^{n+1} - \mathbf{X}^n. \quad (7)$$

This nonlinear system is very complex, and the Jacobian of the system is not available. We use the package SUNDIALS²⁷ to solve the nonlinear system (7) where a Jacobian-free Newton-Krylov (JFNK) method²⁷ is applied.

After \mathbf{X}^{n+1} is known, the velocity \mathbf{u}^{n+1} can be computed by

$$\mathbf{u}^{n+1}(\mathbf{x}, t) = \mathcal{U}\mathcal{L}\mathcal{S}\mathcal{F}\mathbf{X}^{n+1}.$$

Thus the solution is advanced forward by one-step from n to $n + 1$.

The characteristic of our 3D implicit formulation is as follows: (1) the elastic force of the immersed boundary is computed implicitly and the fluid equations are solved explicitly by the lattice Boltzmann method; (2) the massive boundary is handled by the d'Alembert force approach. The advantage of our 3D implicit formulation is that the IB formulation is reduced to a non-linear system of algebraic equations after discretization with the sole unknowns being the position of the immersed boundary, and a general purpose JFNK method may be used for solving the system.

We consider a massive flexible sheet in a 3D rectangular box of moving viscous incompressible fluid. The fluid flows along the x -direction (left-right). The upstream end of the sheet is (virtually) fixed along the y -direction (front-rear), and the sheet is initially placed in an angle with the x - y plane. As the fluid flows by the sheet moves along due to the fluid viscosity subjected to the constraint at the fixed edge. The dimensionless parameters used in our simulations are given as below unless otherwise stated. The length of the square sheet is 1/3. The inflow velocity is 0.01; The constant bending modulus \hat{K}_b is 0.005; The stretching coefficient \hat{K}_s is 200; The stiffness of the virtual spring (for tethering the upstream edge) \hat{K}_{st} is 1.0. The Reynolds number Re is 20–100. The sheet mass density \hat{M} is 0–0.01. The ratio for the fluid domain is 2 : 1 : 1 in x -, y - and z -directions; The lattice size is $120 \times 60 \times 60$.

Many simulations have been performed with various values of Re and \hat{M} . A typical case is reported first: the dimensionless mass density is 0.01; the Reynolds number is $Re = 100$. All other parameters are given as above. The time step is 0.0005. Two typical snapshots

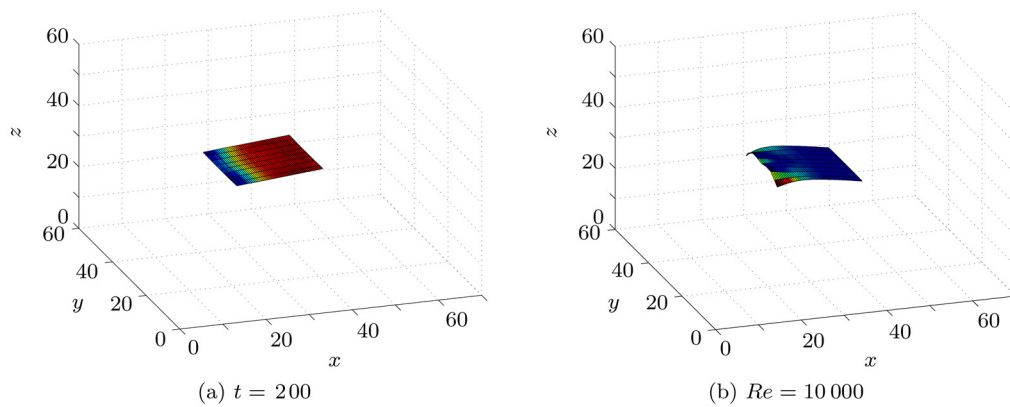


Fig. 1. Snapshots of a massive flexible sheet at $t = 200$ (a) and $t = 10000$ (b) respectively for $Re = 100$.

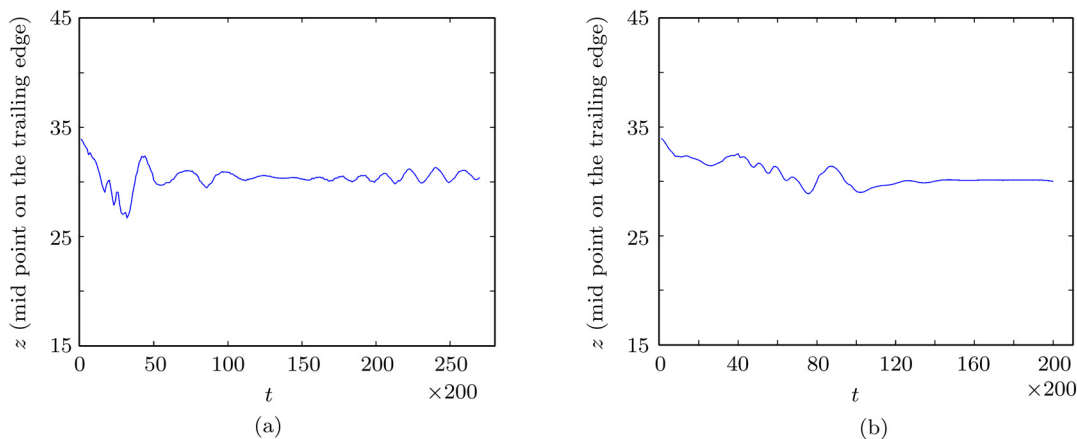


Fig. 2. The z coordinate of the mid point on the trailing edge of the sheet for $Re = 100$ (a) and for $Re = 20$ (b) versus time. The figure shows two distinct stable dynamical states for different Reynolds numbers: the flapping state ($Re = 100$), and the stretched-straight state ($Re = 20$).

of the flexible sheet at $t = 200$ (in LB units) and $t = 10000$ are plotted in Fig. 1. One can see that the sheet still forms an angle with the x - y plane at $t = 200$, and later flaps across the equilibrium position at $t = 10000$.

We plot the z -coordinate of the midpoint on the trailing edge of the sheet evolving over time in Fig. 2 (the left graph). After $t = 30000$, the graph shows a periodic pattern. The dimensionless period and frequency are approximately 0.009 and 111.

In a second typical case, $Re = 20$ and $\hat{M} = 0.01$. A self-sustained flapping state is not seen: the sheet reaches an equilibrium position after $t = 30000$ and does not flap since then (see the right graph in Fig. 2). For a comparison Fig. 2 plots two distinct dynamical stable states: the flapping state for $Re = 100$, and the stretched-straight state for $Re = 20$. This result is in agreement with the findings in Refs. 3, 23, 24.

Figure 3 shows the velocity contour for the x component of flow velocity on the horizontal slice $z = 32$ at $t = 100000$ for the case with $Re = 100$.

Finally, simulations with different values of \hat{M} indicate that the flapping state does not occur for a massless sheet in the range of Reynolds numbers we have consid-

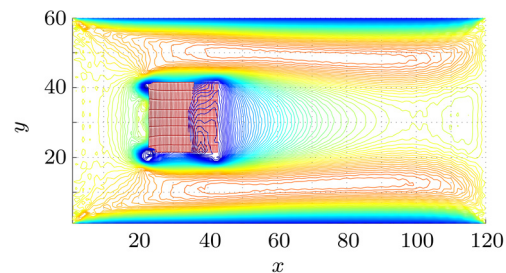


Fig. 3. Velocity (x component) contour on the horizontal slice $z = 32$ at $t = 100000$. $Re = 100$.

ered. It shows that the sheet mass plays a crucial role for self-sustained flapping motion. This is consistent with the findings in Refs. 3, 4, 26.

Through numerical experimentation, we have found that the time step of the implicit method can be at least 10 times greater than the corresponding explicit method. For instance, for the simulation with $Re = 100$, the (nearly) largest dimensionless time step for the explicit method is 5×10^{-5} ; while the implicit method

can take as large as 5×10^{-4} . For each time step the number of Newton's iterations is around 3-4 and for each Newton step the number of linear iterations is around 3-7. Our numerical experiments have showed that the 3D implicit method is more stable than the 3D explicit method. However the current implicit method does not apply any preconditioner in solving the linear system by the generalized minimum residual (GMRES). A good preconditioner is needed to make our implicit method more efficient.

We have developed an implicit immersed boundary method in three dimensions which applies a lattice Boltzmann method (the lattice D3Q19 model) to solve the viscous incompressible Navier-Stokes equations. The highly nonlinear discrete system is solved by a JFNK method. The new method is used to simulate the interaction of a deformable sheet with a 3D viscous incompressible flow. Our preliminary results are consistent with the existing literatures. A good preconditioner for the linear system solver is desired to make the 3D implicit method more efficient.

This work was supported by the US National Science Foundation (DMS-0713718).

1. C. S. Peskin, *Acta Numerica* **11**, 479 (2002).
2. J. M. Stockie, and B. R. Wetton, *J. Comput. Phys.* **154**, 41 (1999).
3. L. Zhu, and C. S. Peskin, *J. Comput. Phys.* **179**, 452 (2002).
4. L. Zhu, and C. S. Peskin, *Phys. Fluids* **15**, 1954 (2003).
5. L. Zhu, *J. Fluid Mech.* **607**, 387 (2008).
6. H. D. Ceniceros, J. E. Fisher, and A. M. Roma, *Journal of Computational Physics* **228**, 7137 (2009).
7. H. D. Ceniceros, and J. E. Fisher, *Journal of Computational Physics* **230**, 5133 (2011).
8. L. J. Fauci, and A. L. Fogelson, *Commun. Pure Appl. Math.* **46**, 787 (1993).
9. T. Y. Hou, and Z. Shi, *J. Comput. Phys.* **227**, 8968 (2008).
10. A. A. Mayo, and C. S. Peskin, *Contemp. Math.* **141**, 261 (1993).
11. E. P. Newren, A. L. Fogelson, and R. D. Guy, et al, *Comput. Methods Appl. Mech. Engrg.* **197**, 2290 (2008).
12. K. Taira, and T. Colonius, *J. Comput. Phys.* **225**, 2118 (2007).
13. C. Tu, and C. S. Peskin, *SIAM J. Sci. Stat. Comput.* **13**, 1361 (1992).
14. Y. Mori, and C.S. Peskin, *Comput. Methods Appl. Mech. Engrg.* **197**, 2049 (2008).
15. J. Hao, and L. Zhu, *Comp. Math. Appl.* **59**, 185 (2010).
16. J. Hao, Z. Li, and S. R. Lubkin, *Discrete and Continuous Dynamical Systems-Series B*, (2011).
17. S. Y. Chen, and G. D. Doolen, *Ann. Rev. Fluid Mech.* **30**, 329 (1998).
18. Z. G. Feng, and E. E. Michaelides, *J. Comput. Phys.* **202**, 20 (2005).
19. Y. Peng, C. Shu, and Y. T. Chew, et al, *Journal of Computational Physics* **218**, 460 (2006).
20. F. B. Tian, H. Luo, and L. Zhu, et al, *J. Comput. Phys.* **230**, 7266 (2011).
21. J. Wu, and C. Shu, *Journal of Computational Physics* **229**, 5022 (2010).
22. A. C. Hindmarsh, P. N. Brown, and K.E. Grant, et al, *Acm Trans. Math. Software* **31**, 363 (2005).
23. M. Shelley, N. Vandenbergh, and J. Zhang, *Physical Review E* **71**, 046302 (2005).
24. J. Zhang, S. Childress, and A. Libchaber, et al, *Nature* **408**, 835 (2000).
25. X. S. Wang, *Computers and Structures*, **85**, 739 (2007).
26. L. Zhu, *Journal of Fluid Mechanics* **635**, 455 (2009).
27. D. A. Knoll, and D.E. Keyes, *J. Comput. Phys.* **193**, 357 (2004).